Implementation of a Position Control System of a Sensorless Synchronous Reluctance Drive

Tian-Hua Liu*, Ming-Tsan Lin**, Ching-Guo Chen*, and Chih-An Tai*

*Department of Electrical Engineering
National Taiwan University of Science and Technology
43 Section 4 Keelung Road Taipei 106, Taiwan , R. O. C
Liu@mail.ntust.edu.tw

**Department of Electrical Engineering
Tung Nan Institute of Technology
Shen-Keng, Taipei 222, Taiwan, R. O. C.
mtlin@mail.tnit.edu.tw

Abstract **- This paper presents a novel position control for a sensorless synchronous reluctance drive system. By measuring the three-phase currents of the motor, a rotor position estimator is achieved. Then, a velocity estimator is derived from the estimated rotor position by using a state estimating technique. Next, a robust position controller is designed to improve the transient and load disturbance responses. A digital signal processor, TMS-320-C30, is used to execute the estimating and control algorithms. To evaluate the performance of the position control system, a moving table is connected with the drive system. The drive system can precisely control the moving table. Experimental results show that the proposed system has good performance.**

I. INTRODUCTION

The synchronous reluctance motor (SRM) has been recognized to have many advantages due to its simple and rugged structure. In addition, there is no winding or magnetic material on its rotor [1]-[2]. Moreover, the SRM is more suitable for a sensorless drive due to its different d- and q-axis inductances. Rotor position estimating techniques have been studied to reduce the cost of the rotor position sensor and to simplify the drive system. Several papers have been investigated to estimate the rotor position of reluctance motors [3]-[4]. Matsuo and Lipo implemented a rotor position estimator by measuring the rate change of the stator currents of an SRM. This method performed well at a low-speed. Unfortunately, the position estimator deteriorated as the speed of the motor was increased. A compensator, therefore, was required. This compensator was related to the motor speeds and initial currents. As a result, it was a three-dimensional compensator, and very difficult to design due to its nonlinear characteristic [4]. Recently, many researchers have studied the sensorless position control of a synchronous reluctance motor. Sul et al. used a combination of a high-frequency current injection and a flux estimation method to achieve a position control of a synchronous reluctance motor [5]. The injection current, however, caused harmonics and torque pulsation as well. Lin and Liu proposed a position control system by measuring the stator currents of the SRM. The system could precisely estimate the shaft position of the motor. This method, however, required a low-pass filter to smooth the estimated velocity. This resulted in a time lag between the real velocity and the estimated velocity and seriously deteriorated performance of the position control system [6].

This paper proposes a new method for the sensorless SRM drive system. By using a state estimation technique, a precise velocity estimator can be obtained. In addition, a robust controller has been designed to improve the performance of the position control system. A moving table is connected with the SRM drive to evaluate the dynamic behavior of the whole closed-loop system. The experimental results show the proposed method performs well. To the best of the authors' knowledge, this proposed sensorless SRM position control system is new.

This research was supported by the National Science Council under grant NSC 89-2213-E-011-071.

II. SYSTEM DESCRIPTION

A. Sensorless Drive System

The block diagram of the SRM drive system investigated is shown in Fig. 1. The system consists of two major parts: the software and the hardware.

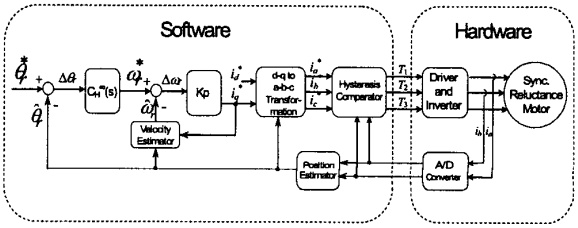

Fig. 1 The block diagram of the position control system.

B. Dynamic Model of a SRM

In the a-b-c axis stationary reference frame, the three-phase voltage of the SRM can be described by the following equations:

$$v_a = r_s i_a + p\lambda_a \quad (1)$$

$$v_b = r_s i_b + p\lambda_b \quad (2)$$

$$v_c = r_s i_c + p\lambda_c \quad (3)$$

where v_a, v_b, v_c are the phase voltages of the SRM, r_s is

0-7803-7474-6/02/$17.00 ©2002 IEEE

the stator winding resistance, i_a, i_b, i_c are stator currents, p is the differential operator, and $\lambda_a, \lambda_b, \lambda_c$ are the flux linkages of the three phases. The flux linkages can be expressed as

$$\lambda_a = L_{aa} i_a + L_{ab} i_b + L_{ac} i_c \quad (4)$$

$$\lambda_b = L_{ba} i_a + L_{bb} i_b + L_{bc} i_c \quad (5)$$

$$\lambda_c = L_{ca} i_a + L_{cb} i_b + L_{cc} i_c \quad (6)$$

where L_{aa}, L_{bb}, L_{cc} are the a-phase, b-phase, and c-phase self-inductances. $L_{ab}, L_{ac}, L_{ba}, L_{bc}, L_{ca}$, and L_{cb} are the mutual inductances between the stator windings. The self and mutual inductances for a SRM can be expressed as [4]

$$L_{aa} = L_{ls} + L_A - L_B \cos 2\theta_r \quad (7)$$

$$L_{bb} = L_{ls} + L_A - L_B \cos(2\theta_r + \frac{2}{3}\pi) \quad (8)$$

$$L_{cc} = L_{ls} + L_A - L_B \cos(2\theta_r - \frac{2}{3}\pi) \quad (9)$$

$$L_{ab} = L_{ba} = -\frac{1}{2} L_A - L_B \cos(2\theta_r - \frac{2}{3}\pi) \quad (10)$$

$$L_{bc} = L_{cb} = -\frac{1}{2} L_A - L_B \cos 2\theta_r \quad (11)$$

$$L_{ca} = L_{ac} = -\frac{1}{2} L_A - L_B \cos(2\theta_r + \frac{2}{3}\pi) \quad (12)$$

where L_{ls} is the leakage inductance, L_A is the parameter which is unrelated to the rotor position, L_B is the parameter which is related to the rotor position, and θ_r is the electrical rotor position of the motor. After the stator currents are transformed from the a-b-c axis to the d-q axis, the electro-magnetic torque expressed in the d-q synchronous frame is

$$T_e = \frac{3}{2} \frac{P_0}{2} (3 L_B) i_d i_q \quad (13)$$

where T_e is the electro-magnetic torque of the motor, P_0 is the number of poles of the motor, i_d is the d-axis equivalent current, and i_q is the q-axis equivalent current.

III. SENSORLESS TECHNIQUE

From the dynamic equations of the SRM, it is possible to estimate the rotor position by using a state estimator. This method, however, is very complicated and difficult to implement. From equations (1)-(6), we can observe that the differential value of the stator current is related to the inductances of the motor. In addition, the inductances of the motor are a function of the rotor position as well. As a result, it is possible to measure the current deviations and then estimate the rotor position using the measured current derivations. This paper, therefore, proposes a sensorless technique by only detecting the stator currents. The detailed analysis follows.

A. Shaft Position Estimator

The synchronous motor is driven by a voltage- source current-regulated inverter. The inverter has eight switching states including six conduction modes and two freewheeling modes [4]. In order to explain the basic principle, only three conduction modes are discussed in detail. The other operating modes can be analyzed by using the same method. Fig. 2 shows the conduction mode A^+. In this mode, the switches T_1, T_2', and T_3' are turned on. Then, the voltage and current equations can be expressed as

$$V_{dc} = v_a - v_b \quad (14)$$

$$v_b = v_c \quad (15)$$

$$i_a = -(i_b + i_c) \quad (16)$$

Because the changes of voltage drops of the stators resistances are small when the stator currents vary between active modes and freewheeling modes, the voltage drops of the stator resistances can be neglected. And substituting (1)-(2) into (14), we can easily obtain

$$V_{dc} = p\lambda_a - p\lambda_b \quad (17)$$

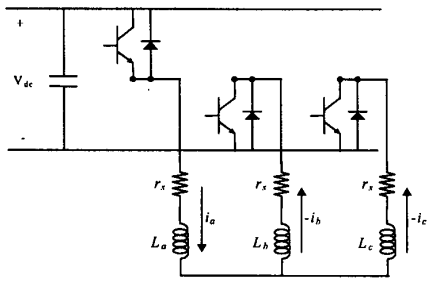

Fig. 2 The illustrated conduction mode A^+

After that, by using (4) - (5) to express the flux linkages λ_a and λ_b, we can obtain

$$V_{dc} = [(L_{aa} pi_a + L_{ab} pi_b + L_{ac} pi_c) - (L_{ba} pi_a + L_{bb} pi_b + L_{bc} pi_c)] + [(i_a dL_{aa}/d\theta_r + i_b dL_{ab}/d\theta_r + i_c dL_{ac}/d\theta_r) - (i_a dL_{ba}/d\theta_r + i_b dL_{bb}/d\theta_r + i_c dL_{bc}/d\theta_r)]\,\omega_r \quad (18)$$

Neglecting the voltage drop of the resistance and then substituting (2)-(3) into (15), we can obtain the following equation:

$$p\lambda_b = p\lambda_c \quad (19)$$

After substituting (5)-(6) into (19) and letting $L_{ab} = L_{ba}$, $L_{bc} = L_{cb}$, and $L_{ca} = L_{ac}$, we can derive

$$0=[(L_{ab}-L_{ac})pi_a+(L_{bb}-L_{bc})pi_b+(L_{bc}-L_{cc})pi_c) + \omega_r[(\frac{dL_{ab}}{d\theta_r}-\frac{dL_{ac}}{d\theta_r})i_a+(\frac{dL_{bb}}{d\theta_r}-\frac{dL_{bc}}{d\theta_r})i_b+(\frac{dL_{bc}}{d\theta_r}-\frac{dL_{cc}}{d\theta_r})i_c] \quad (20)$$

Considering the freewheeling mode (mode 0), the three-phase windings are shorted and disconnected from the input dc voltage. As a result, we can substitute $v_{dc} = 0\,\mathrm{V}$ into equation (18) and (20), and obtain the following equations, respectively:

$$0=\left[(L_{aa}-L_{ab})\frac{di_a}{dt}|_{\mathrm{mod}\,e0}+(L_{ab}-L_{bb})\frac{di_b}{dt}|_{\mathrm{mod}\,e0}+(L_{ac}-L_{bc})\frac{di_c}{dt}|_{\mathrm{mod}\,e0}\right] + \omega_r\left[\left(\frac{dL_{aa}}{d\theta_r}-\frac{dL_{ab}}{d\theta_r}\right)i_a+\left(\frac{dL_{ab}}{d\theta_r}-\frac{dL_{bb}}{d\theta_r}\right)i_b+\left(\frac{dL_{ac}}{d\theta_r}-\frac{dL_{bc}}{d\theta_r}\right)i_c\right] \quad (21)$$

and

$$0=\left[(L_{ab}-L_{ac})\frac{di_a}{dt}|_{\mathrm{mod}\,e0}+(L_{bb}-L_{bc})\frac{di_b}{dt}|_{\mathrm{mod}\,e0}+(L_{bc}-L_{cc})\frac{di_c}{dt}|_{\mathrm{mod}\,e0}\right] + \omega_r\left[\left(\frac{dL_{ab}}{d\theta_r}-\frac{dL_{ac}}{d\theta_r}\right)i_a+\left(\frac{dL_{bb}}{d\theta_r}-\frac{dL_{bc}}{d\theta_r}\right)i_b+\left(\frac{dL_{bc}}{d\theta_r}-\frac{dL_{cc}}{d\theta_r}\right)i_c\right] \quad (22)$$

Then, by substituting (21) into (18), it is easy to obtain:

$$V_{dc}=\left[(L_{aa}-L_{ab})\left(\frac{di_a}{dt}|_{\mathrm{mod}\,eA+}-\frac{di_a}{dt}|_{\mathrm{mod}\,e0}\right)+(L_{ab}-L_{bb})\left(\frac{di_b}{dt}|_{\mathrm{mod}\,eA+}-\frac{di_b}{dt}|_{\mathrm{mod}\,e0}\right)\right] + (L_{ac}-L_{bc})\left(\frac{di_c}{dt}|_{\mathrm{mod}\,eA+}-\frac{di_c}{dt}|_{\mathrm{mod}\,e0}\right) \quad (23)$$

Next, by substituting (22) into (20), it is easy to obtain:

$$0=\left[(L_{ab}-L_{ac})\left(\frac{di_a}{dt}|_{\mathrm{mod}\,eA+}-\frac{di_a}{dt}|_{\mathrm{mod}\,e0}\right)+(L_{bb}-L_{bc})\left(\frac{di_b}{dt}|_{\mathrm{mod}\,eA+}-\frac{di_b}{dt}|_{\mathrm{mod}\,e0}\right) + (L_{bc}-L_{cc})\left(\frac{di_c}{dt}|_{\mathrm{mod}\,eA+}-\frac{di_c}{dt}|_{\mathrm{mod}\,e0}\right)\right] \quad (24)$$

By differentiating the left side and right side of (16), it is easy to obtain

$$pi_a = -(pi_b + pi_c) \quad (25)$$

From (23)-(25), we can derive

$$\frac{di_a}{dt}|_{\mathrm{mod}\,eA+}-\frac{di_a}{dt}|_{\mathrm{mod}\,e0}=(2L_{bc}-L_{bb}-L_{cc})V_{dc}/\Delta \quad (26)$$

$$\frac{di_b}{dt}|_{\mathrm{mod}\,eA+}-\frac{di_b}{dt}|_{\mathrm{mod}\,e0}=(L_{ab}-L_{ac}-L_{bc}+L_{cc})V_{dc}/\Delta \quad (27)$$

$$\frac{di_c}{dt}|_{\mathrm{mod}\,eA+}-\frac{di_c}{dt}|_{\mathrm{mod}\,e0}=(L_{ab}+L_{bc}-L_{ac}-L_{bb})V_{dc}/\Delta \quad (28)$$

where

$$\Delta=(L_{aa}-L_{ab}-L_{ac}+L_{bc})^2-(L_{aa}-2L_{ab}+L_{bb})(L_{aa}-2L_{ac}+L_{cc}) \quad (29)$$

By using the same method, it is not difficult to derive

$$\frac{di_a}{dt}|_{\mathrm{mod}\,eB+}-\frac{di_a}{dt}|_{\mathrm{mod}\,e0}=(L_{ab}-L_{ac}-L_{bc}+L_{cc})V_{dc}/\Delta \quad (30)$$

$$\frac{di_b}{dt}|_{\mathrm{mod}\,eB+}-\frac{di_b}{dt}|_{\mathrm{mod}\,e0}=(2L_{ac}-L_{aa}-L_{cc})V_{dc}/\Delta \quad (31)$$

$$\frac{di_c}{dt}|_{\mathrm{mod}\,eB+}-\frac{di_c}{dt}|_{\mathrm{mod}\,e0}=(L_{aa}+L_{bc}-L_{ab}-L_{ac})V_{dc}/\Delta \quad (32)$$

$$\frac{di_a}{dt}|_{\mathrm{mod}\,eC+}-\frac{di_a}{dt}|_{\mathrm{mod}\,e0}=(L_{ac}+L_{bb}-L_{ab}-L_{bc})V_{dc}/\Delta \quad (33)$$

$$\frac{di_b}{dt}|_{\mathrm{mod}\,eC+}-\frac{di_b}{dt}|_{\mathrm{mod}\,e0}=(L_{ab}+L_{ac}-L_{aa}-L_{bc})V_{dc}/\Delta \quad (34)$$

$$\frac{di_c}{dt}|_{\mathrm{mod}\,eC+}-\frac{di_c}{dt}|_{\mathrm{mod}\,e0}=(L_{aa}-2L_{ab}+L_{bb})V_{dc}/\Delta \quad (35)$$

By substituting (7)-(12) into (26)-(35), one can obtain

$$Di_{a\mathrm{mode}\,A+}=\frac{di_a}{dt}_{\mathrm{mode}\,A+}-\frac{di_a}{dt}_{\mathrm{mode}\,0}=\frac{4V_{dc}\left(\frac{2}{3}L_{ls}+L_A+\cos(2\theta_r)L_B\right)}{(2L_{ls}+3(L_A-L_B))(2L_{ls}+3(L_A+L_B))} \quad (36)$$

$$Di_{b\mathrm{mode}B+}=\frac{di_b}{dt}_{\mathrm{mode}B+}-\frac{di_b}{dt}_{\mathrm{mode}0}=\frac{2V_{dc}\left(2(\frac{2}{3}L_{ls}+L_A)-\left(\cos(2\theta_r)+\sqrt{3}\sin(2\theta_r)\right)L_B\right)}{(2L_{ls}+3(L_A-L_B))(2L_{ls}+3(L_A+L_B))} \quad (37)$$

$$Di_{cmodeC+} = \frac{di_c}{dt}_{modeC+} - \frac{di_c}{dt}_{mode0} = \frac{2V_{dc}\left(2\left(\frac{2}{3}L_{ls}+L_A\right)+\left(-cos(2\theta_r)+\sqrt{3}sin(2\theta_r)\right)L_B\right)}{(2L_{ls}+3(L_A-L_B))(2L_{ls}+3(L_A+L_B))} \quad (38)$$

To estimate the rotor position, it is better to transform the data from the a-b-c axis to the α-β axis. The transformation can be expressed as

$$\begin{bmatrix} Di_\alpha \\ Di_\beta \end{bmatrix} = \begin{bmatrix} 1 & -\frac{1}{2} & -\frac{1}{2} \\ 0 & \frac{\sqrt{3}}{2} & -\frac{\sqrt{3}}{2} \end{bmatrix} \begin{bmatrix} Di_a \\ Di_b \\ Di_c \end{bmatrix} \quad (39)$$

Then, by substituting (36)-(38) into (39), the pseudo variables can be shown as

$$Di_\alpha = \frac{6V_{dc}L_B cos(2\theta_r)}{(2L_{ls}+3(L_A-L_B))(2L_{ls}+3(L_A+L_B))} \quad (40)$$

and

$$Di_\beta = \frac{6V_{dc}L_B sin(2\theta_r)}{(2L_{ls}+3(L_A-L_B))(2L_{ls}+3(L_A+L_B))} \quad (41)$$

The rotor angle, therefore, is expressed as

$$\theta_T = \tan^{-1}\frac{Di_\beta}{Di_\alpha} = 2\theta_r \quad (42)$$

To obtain the electrical rotor angle, a program has been developed to map the double value of the electrical rotor angle, which is shown in (42), into the electrical rotor angle.

B. Velocity Estimator

In this paper, a velocity estimator has been designed to predict the velocity of the motor. The velocity estimator has a good tracking ability and a good steady-state characteristic. The input of the velocity estimator includes the estimated position angle and the q-axis current of the motor. In this paper, the q-axis current command is used to replace the q-axis current because they are very close. The internal states of the velocity estimator include $\hat{x}_1$, $\hat{x}_2$, and $\hat{x}_3$. The drive system was controlled under field- oriented control. Neglecting the external load T_L, one can derive the simplified model as

$$\begin{bmatrix} \dot{x}_1 \\ \dot{x}_2 \\ \dot{x}_3 \end{bmatrix} = \begin{bmatrix} 0 & 1 & 0 \\ 0 & 0 & \frac{1}{J} \\ 0 & 0 & 0 \end{bmatrix} \begin{bmatrix} x_1 \\ x_2 \\ x_3 \end{bmatrix} + \begin{bmatrix} 0 \\ \frac{K_t}{J} \\ 0 \end{bmatrix} i_q = AX + Bu \quad (43)$$

and

$$y = \begin{bmatrix} 1 & 0 & 0 \end{bmatrix} \begin{bmatrix} x_1 \\ x_2 \\ x_3 \end{bmatrix} = CX \quad (44)$$

where x_1 is the shaft position of the motor, x_2 is the velocity of the motor, and x_3 is the pseudo variable, which is an isolated variable and has a dynamic equation of $\dot{x}_3 = x_3 = 0$, and y is the output of the estimator, which is equal to $\hat{\theta}_r$.

Then, assuming $J = \hat{J}$ and $K_t = \hat{K}_t$, the state estimator is expressed as

$$\begin{bmatrix} \dot{\hat{x}}_1 \\ \dot{\hat{x}}_2 \\ \dot{\hat{x}}_3 \end{bmatrix} = \begin{bmatrix} 0 & 1 & 0 \\ 0 & 0 & \frac{1}{\hat{J}} \\ 0 & 0 & 0 \end{bmatrix} \begin{bmatrix} \hat{x}_1 \\ \hat{x}_2 \\ \hat{x}_3 \end{bmatrix} + \begin{bmatrix} 0 \\ \frac{\hat{K}_t}{\hat{J}} \\ 0 \end{bmatrix} i_q + \begin{bmatrix} K_1 \\ K_2 \\ K_3 \end{bmatrix} (\hat{\theta}_r - \hat{x}_1) = A\hat{X} + Bu + K(y - C\hat{X}) \quad (45)$$

and

$$\hat{y} = \begin{bmatrix} 1 & 0 & 0 \end{bmatrix} \begin{bmatrix} \hat{x}_1 \\ \hat{x}_2 \\ \hat{x}_3 \end{bmatrix} = C\hat{X} \quad (46)$$

where $\hat{x}_1$, $\hat{x}_2$, and $\hat{x}_3$ are estimated states.

C. Robust Controller Design

The object of the H^∞ controller is to minimize the criterion of the following form

$$\sup_\omega \left[\left|V(j\omega)S(j\omega)\right|^2 + \left|W(j\omega)T(j\omega)\right|^2\right] \quad (47)$$

where V and W are weighting functions based on the designer's choice, S is the sensitivity function, and T is the closed-loop transfer function. The transfer function T is a complementary of the sensitivity function S. In this paper, the weighting functions are selected as [7]:

$$V(s)V(-s) = \frac{1+(\tau_1 s)^4}{(\tau_1 s)^4} \quad (48)$$

and

$$W(s) = (\tau_2 s)^2 \tag{49}$$

where τ_1 and τ_2 are tuning parameters. Let $\alpha = (\tau_2 / \tau_1)^4$. The weighting function *V(s)* is used to reject constant disturbances and attenuate very-low-frequency disturbances. On the other hand, the weighting function *W(s)* is used to obtain a proper closed-loop transfer function.

The SRM is simplified as a linear second-order system. The transfer function of the minor velocity loop system can be expressed as

$$P(s) = \frac{K_p K_t}{Js^2 + K_p K_t s} = \frac{K_0}{s^2 + K_0 s} \tag{50}$$

where K_p is the proportional controller of the velocity loop, and K_0 is the product of K_p and K_t. Based on the design rules given in paper [7], the position-loop H^∞ controller is of the form

$$C_{H^\infty}(s) = \frac{(K_0 + s)(\xi_0 + \xi_1 s)}{K_0 \tau_1^{\,2} s(\theta_0 + \theta_1 s)} \tag{51}$$

where ξ_0, ξ_1 θ_0, and θ_1 are the parameters of the controller and are obtained by equating the coefficients of equal powers in s for the following equation:

$$\lambda\{[s^2(\theta_1 s + \theta_0) + (\xi_1 s + \xi_0)][s^2(-\theta_1 s + \theta_0) + (-\xi_1 s + \xi_0)]\} = [(\frac{1}{\tau_1^4} + s^4)(\theta_1 s + \theta_0)(-\theta_1 s + \theta_0) + \alpha s^4 (\xi_1 s + \xi_0)(-\xi_1 s + \xi_0)]\tau_1^4 \tag{52}$$

To solve ξ_0, ξ_1 θ_0, and θ_1 in (52), let θ_1=1 and the solutions are

$$\theta_0 = \sqrt{\frac{\lambda^4 - \lambda^2 - \alpha}{2\alpha\lambda}} \tag{53}$$

$$\xi_1 = \sqrt{\frac{\lambda^2 - 1}{\alpha}} \tag{54}$$

$$\xi_0 = \sqrt{\frac{\lambda^4 - \lambda^2 - \alpha}{2\alpha\lambda^3}} \tag{55}$$

with λ and α satisfying

$$(\lambda^4 - \lambda^2 - \alpha)^2 - 4\lambda^5\sqrt{(\lambda^2 - 1)\alpha} = 0 \tag{56}$$

According to (56), for each α, the parameter λ can be uniquely determined by using numerical methods. For simplicity, α is fixed to a small number leaving τ_1 the only tuning parameter in equation (51).

IV. EXPERIMENTAL RESULTS

The proposed sensorless algorithm was evaluated by experimental results. Fig. 3 shows the relative measured position angles. The estimated angle is close to the real angle. In addition, no initial obvious estimated error appears. Fig. 4 shows the measured position responses of different position commands. The responses are smooth and fast. The position controller is selected as $C_{H^\infty}(s) = (504 + s)(112 + 159s)$ $/(5164s(113 + s))$. Fig. 5 shows the position response at 5 mm with a 2 N.m external load. Fig. 6 shows the responses of the velocity estimators. The proposed estimator can obtain a precise velocity because the time-lag problem is improved by using the state estimating technique. In addition, the proposed method performs better than the traditional estimator by using differential method. The real velocity is measured by using an encoder with 8000 pulses per revolution. Fig. 7 shows the measured position response of a triangle command. The position tracks its command well.

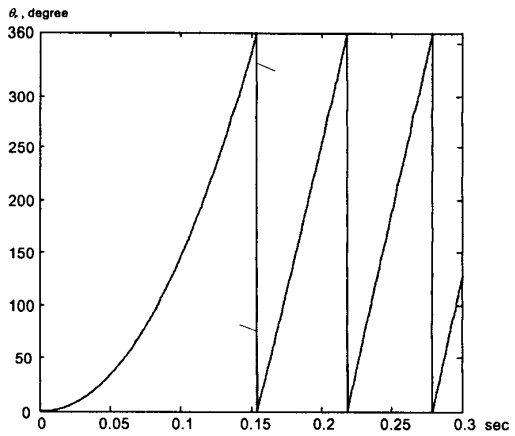

Fig. 3 The measured steady-state position angles

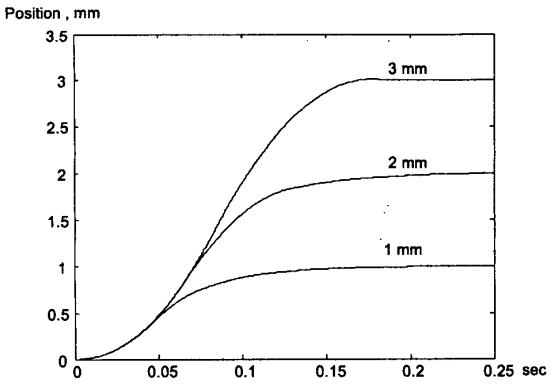

Fig. 4 The measured position responses.

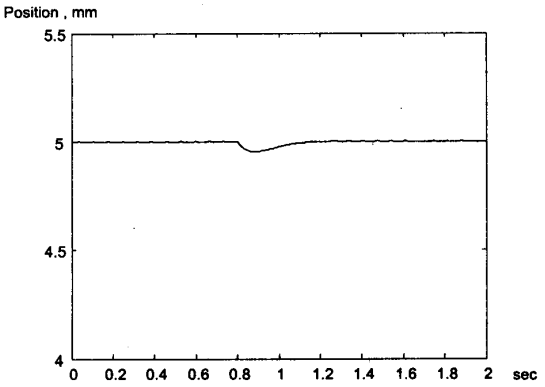

Fig. 5 The measured load disturbance responses

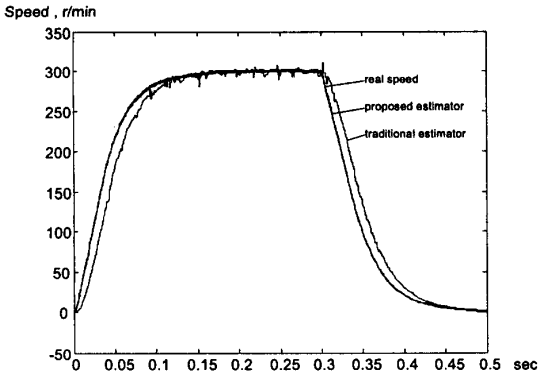

Fig. 6 The tracking responses of different velocity estimators.

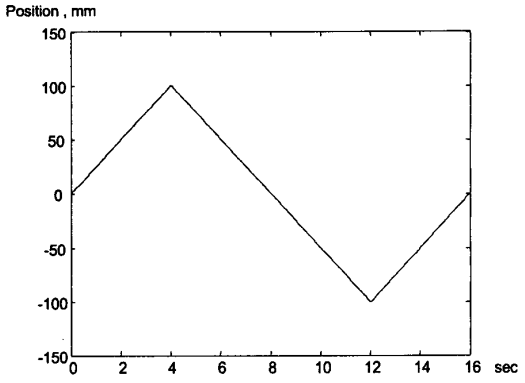

Fig.7 The measured responses of a triangle command

V. CONCLUSIONS

In this paper, a systematic method for implementing a position control of a sensorless synchronous reluctance drive system is presented. By measuring the rate change of the stator current, the rotor position of the motor was accurately determined. A fully digital, multi-rate, digital signal processor based control system was implemented. The sensorless drive system performed well.

VI. REFERENCES

[1] T. A. Lipo, "Recent progress in the development of solid-state ac motor drives," *IEEE Trans. Power Electron.*, vol. 3, no. 2, Apr. 1988, pp. 105-117.

[2] B. K. Bose, "Technology trends in microprocessor control of electrical machines," *IEEE* Trans. *Ind. Electron.*, vol. 35, no. 1, Feb. 1988, pp. 160-177.

[3] M. S. Arefeen, M. Ehsani, and T. A. Lipo, "Sensorless position measurement in synchronous reluctance motor," *IEEE Trans. Power Electron.*, vol. 9, no. 6, Nov. 1994, pp. 624-630.

[4] T. Matsuo and T. A. Lipo, "Rotor position detection scheme for synchronous reluctance motor based on current measurements," *IEEE Trans. Ind. Applicat.*, vol. 31, no. 4, July/Aug. 1995, pp. 860-868.

[5] J. I. Ha, S. J. Kang, and S. K. Sul, "Position-controlled synchronous reluctance motor without rotational transducer," *IEEE Trans. Ind. Applicat.*, vol. 35, no. 6, Nov./ Dec. 1999, pp. 1393-1398.

[6] M. T. Lin and T. H. Liu, "Sensorless synchronous reluctance drive with standstill starting," *IEEE Trans. Aero. and Electron. Sys.*, vol. 36, no. 4, Oct. 2000, pp. 1232-1241.

[7] H. Kwakernaak, "Minmax frequency domain performance and robustness optimization of linear feedback systems," *IEEE Trans. Automat. Contr.*, vol. 30, no. 10, Oct. 1985, pp. 994-1004.